Influence of Surface Modifiers on Hydrothermal Synthesis of $K_xNa_{(1-x)}NbO_3$

L. Ramajo [1]*, F. Rubio-Marcos [2], A. Del Campo [2], J. F. Fernández [2], M.S. Castro [1], R. Parra [1]

(1) Institute of Research in Materials Science and Technology (INTEMA) (CONICET – University of Mar del Plata), J. B. Justo 4302, B7608FDQ - Mar del Plata, Argentina.

(2) Electroceramic Department, Instituto de Cerámica y Vidrio, CSIC, Kelsen 5, 28049, Madrid, Spain.

Abstract

The synthesis of Potassium-Sodium Niobate Lead-free Piezoelectric Ceramics has been widely studied during the past decade because of the promising industrial application of these materials. We here report the effect of different additives or surface modifiers (such as cetyltrimethylammonium bromide, hexamethylenetetramine, and Triton X-100) on the synthesis of $K_xNa_{1-x}NbO_3$ by a hydrothermal process. To achieve this purpose, ceramics powders are prepared using a 0.6 KOH/NaOH ratio, with a total OH^- concentration of 8N under hydrothermal conditions at 200°C. Surface modifiers are used aiming to avoid agglomeration, to modify the particle surface morphology and to improve the sample density after sintering. It is worth to note that the potassium concentration in $K_xNa_{(1-x)}NbO_3$ was increased by the incorporation of the surface modifiers. In this way, $K_xNa_{1-x}NbO_3$–based ceramics exhibit enhanced electrical properties.

KEYWORDS: Lead-free, Hydrothermal, $K_xNa_{1-x}NbO_3$.

*Author to whom correspondence should be addressed: Tel. +54-223-4816600 (ext. 238) e-mail: lramajo@fi.mdp.edu.ar

1. Introduction

The use of lead-free piezoelectric materials has gained much attention in recent years. Sodium potassium niobate $K_xNa_{1-x}NbO_3$ (KNN), a possible candidate for replacing lead based piezoelectrics ($Pb(Zr_xTi_{1-x})O_3$ or PZT), is appealing for potential piezoelectric applications because of its relatively low dielectric permittivity, high electro-mechanical coupling coefficient and lack of environmental hazard [1-2]. However, this system also suffers from a number of uncertainties and drawbacks, for example, the pure KNN ceramics are difficult to be densified by conventional sintering method due to volatility of alkali components and instability of crystal phase at high temperature [3-4].

In the process of preparing ceramics by a solid-state route, the alkaline carbonates used commonly as raw materials exhibit hygroscopic behavior, which makes it difficult to achieve the desired stoichiometry because reagents may not react completely. Introducing new synthetic methods, such as wet-chemical procedures can effectively avoid these shortcomings [5]. Zeng *et al.* [6] and Xu *et al.* [7] have prepared KNN powders using the molten-salt method and sol–gel processing. Alternatively, the hydrothermal method is a wet chemical technique that leads to crystalline complex oxide powders [8]. $KNbO_3$ and $NaNbO_3$ powders have also been successfully synthesized under hydrothermal conditions [9–12]. However, the hydrothermal synthesis of the (K, Na)NbO_3 solid solution, especially of the $K_{0.5}Na_{0.5}NbO_3$ composition, has been reported to a lesser extent in literature. The reason seems to be that $KNbO_3$ and $NaNbO_3$ always form separately under hydrothermal conditions. It is known that Na reacts more readily with Nb to form $NaNbO_3$ than K to form $KNbO_3$ [13], then the conventional hydrothermal method presents certain difficulties to yield pure phases and compositional homogeneous products in one step, making it necessary to perform further thermal treatments [14].

In the high temperature mixing method (HTMM), the starting solutions or raw materials are mixed at the desired reaction temperature. This method bears the advantage to avoid the formation of intermediate phases during the heating process under hydrothermal conditions. In addition, the crystallinity of the obtained powders can be also enhanced. Regarding the use of additives in hydrothermal synthesis of KNN, few articles report the surfactant effects. Two interesting papers showed the influence of SDBS (sodium dodecylbenzenesulfonate), an anionic surfactant, on the size and morphology of KNN particles [13, 15]. However, how these additives may influence the electrical properties of final devices is still unknown.

In this work, $K_xNa_{(1-x)}NbO_3$ is synthesized by a hydrothermal method using different surface modifiers in order to improve the microstructural and electrical properties of KNN-based ceramics. Namely, cetyltrimethylammonium bromide (cationic surfactant), Triton X-100 (non-ionic surfactant) and hexamethylenetetramine are tested in this study. To achieve this purpose, the ceramics powders are prepared using a 0.6 NaOH/KOH ratio, with an 8N hydroxide (OH^-) concentration under hydrothermal conditions. The addition of the modifiers on the hydrothermal synthesis process resulted in structural changes of the perovskite lattice. The observed structural changes were ascribed to the diffusion of potassium within the (KNa)NbO_3

perovskite lattice, by means of which the K content in the structure is increased. This increase in the K concentration led to samples with improved electrical properties.

2. Experimental

The precursors used were analytic grade Nb_2O_5 (Aldrich, 99.8%), NaOH and KOH (BioPack, 99.8%), cetyltrimethylammonium bromide (CTAB), Triton X-100, and hexamethylenetetramine (HMTA). Aqueous solutions of KOH and NaOH were mixed in a 0.6 NaOH/KOH ratio and adjusted to a final 8N OH^- concentration. The resulting alkaline solution was transferred to a Teflon lined stainless-steel autoclave along with 1g of Nb_2O_5 and the selected additive (40mg CTAB; 530mg HMTA or 323mg Triton X-100). The reactor was heated to the desired temperature (200 ºC) with constant stirring for 3h.

The crystalline phases were assessed by X-ray diffraction using a Philips PW1050/25 diffractometer running with CuK_α radiation at 40kV and 30mA. The particle size and morphology of the powder ceramics obtained by hydrothermal reaction were evaluated using a Scanning Electron Microscope, SEM, (JEOL JSM-6460LV microscope). Moreover, the microstructure was also evaluated on polished and thermally etched samples (950 ºC for 5 min) by SEM. The composition of obtained powders was evaluated by X-ray Fluorescence using a MiniPal 2 EDXRF – Spectrometer. Raman spectra were acquired at room temperature with a Renishaw in Via microscope by means of the 514 nm Ar-ion laser line (50 mW nominal power) with a diffraction grating of 2400 lines/mm**.**

In order to characterize the electrical properties of the synthesized material, powders were uniaxially pressed into disks of 5 mm and 0.6 mm in diameter and thickness, respectively, and sintered at 1125 ºC in a Carbolite RHF17 with heating and cooling rates of 5ºC/min. The microstructural characterization of sintered and polished samples was completed by SEM (Jeol JSM-6460LV) and the apparent density measured by the Archimedes method.

To characterize the dielectric and piezoelectric properties, the ceramic specimens were polished and coated with silver paint on the upper and bottom surfaces and fired at 700 °C for 20 min. The temperature dependence of permittivity was measured using an impedance analyzer (HP4294A, Agilent) in the frequency range 100 Hz–1 MHz and the temperature range 30–500 °C, using a heating rate of 2 °C min^{-1}. Finally, the ferroelectric nature of these ceramics was determined using a hysteresis meter (RT 6000 HVS, RADIANT Technologies). In order to test the piezoelectric constant, samples were polarized under a direct current (dc) electric field of 40 kV cm^{-1} in a silicone oil bath at 25 °C for 30 min. The piezoelectric constant d_{33} was measured using a piezo d_{33} meter (YE2730A d_{33} METER, APC International).

3. Results and discussion

XRD patterns of KNN synthesized using different additives (CTA, HMTA and Triton X-100) and sintering at 1125ºC are shown in Figure 1. The diffraction patterns show that these systems are close to the $K_{0.10}Na_{0.90}NbO_3$ (JCPDS 74-2025) and $K_{0.65}Na_{0.35}NbO_3$ (JCPDS 77-0038) phases. According to the XRD patterns, it can be suggested that the powders obtained with the addition of Triton X-100 as surface modifier present higher K^+ concentration. The diffraction peaks between 44.75° and 46.5° 2θ, corresponding to the (400) and (040) planes of the $K_xNa_{1-x}NbO_3$ monoclinic structure (Fig. 1) are analysed in detail. Differences between samples are observed depending on the additive used, being the CTAB and HMTA the most influencing additives. A slight shift in the peak at 46.3°2θ was only observed when Triton X-100 was used. The change in the peak shape may suggest the existence of more than one $K_xNa_{1-x}NbO_3$ phase, probably $K_{0.10}Na_{0.90}NbO_3$ and $K_{0.65}Na_{0.35}NbO_3$. Therefore, using the monoclinic point group C2/M, a limited evolution of the lattice parameters is determined: a = 3.918 Å, b = 3.889 Å, c = 3.923 Å, and β = 89.47° (c/a = 1.0013), for systems without additives, and a = 3.918 Å, b = 3.889 Å, c = 3.924 Å, and β = 89.47° (c/a = 1.0016) for CTAB; a = 3.918 Å, b = 3.883 Å, c = 3.9236 Å, and β = 89.52° (c/a = 1.0014) for HTMA; a = 3.919 Å, b = 3.894 Å, c = 3.933 Å, and β = 89.51° (c/a = 1.0036) for Triton X-100. Then, it can be seen that the additives increase slightly the tetragonality.

In order to obtain additional structural information of the samples synthesized with and without additives, Raman spectra were recorded at room temperature in the 100 to 900cm^{-1} range (Figure 2a). All systems show four main vibration bands at 250, 560, 615 and 870cm^{-1}, which can be identified as ν_5, ν_2, ν_1 and ν_{1+5}, respectively, for $K_xNa_{1-x}NbO_3$ systems. The band at 160cm^{-1} is due to the vibration modes of the octahedral NbO_6, while the bands below 160 cm^{-1} are due to the translational modes of K^+ and Na^+ ions [16]. Interestingly, samples for which additives were used showed lower intensity and increased band breath, which could be attributed to a decrease in particle size.

Figure 2b shows the effects of additives on the ν_1 and ν_2 vibration modes. An increase in ν_1 is observed whereas ν_2 decreases with the additives. The ν_1 increases due to the decrease in the constant force strength caused by the lengthening of the distance between B^{5+} type ions and the corresponding coordinated oxygen [17]. In general, the obtained samples presented similar ν_1 values, which suggests that the bond strength is independent of the additive. Changes can be ascribed to variations or small distortions in the NbO_6 octahedra and crystalline structure, in turn associated with the decrease in particle size [18]. The shift to higher wavenumbers on ν_1 may indicate a decrease in the length and an increase in the strength of Nb-O bond. From XRD and Raman results, it is concluded that the additives improved the incorporation of K in the $K_xNa_{1-x}NbO_3$ lattice. Moreover, the band at 870cm^{-1}, absent in the spectrum of $NaNbO_3$, indicates the incorporation of K in the network [18].

Figures 3(a-e) show SEM micrographs along with X-ray fluorescence (XRF) analysis of the powders obtained by hydrothermal reaction using different additives (CTA, HMTA and Triton X-100). Particles are cubic shaped, which is

expected for KNN-based ceramics, and show average sizes about 1 μm^3. Powders synthesized using CTAB and Triton X-100 showed smaller particle sizes. Although aggregates of small particles are present, secondary nucleation processes have not apparently occurred. XRF results shown in Fig. 3e demonstrate that the surfactants increased the potassium concentration in the structure. The highest values of K are obtained with the addition of Triton X-100 (0.94% wt). From the results showed in Table 1 we can assume that systems with higher potassium concentration (similar to $K_{0.5}Na_{0.5}NbO_3$ composition) will have improved dielectric properties.

Figures 4(a-c) show SEM micrographs of the sintered samples prepared from powders obtained with different additives. SEM images show sintered ceramics with low porosity, in which pores are located mainly at grain boundaries and triple points. Triple points close to 120º indicate the final stage of sintering where pores are removed by diffusion processes. The incorporation of K^+ ions into the composition induces the evolution of grain morphology to nearly rectangular shaped grains with triple point angles of 90º. The secondary nucleation of small crystals improved the surface diffusion mechanisms that promoted the formation of the characteristic rectangular KNN grains. Considering the usual densification problems of KNN, these samples present a high degree of densification [19-20]. High density values are attained in virtue of the synthesized powder, whose nanosized particles determine its reactivity. Furthermore, the sample density does not change due to the additive effect or K^+ content as shown in Table 1. However, a change of the average grain size and grain morphology was observed due to additive effect, as depicted in Figs. 4(a and c). Samples are composed of grains from 5 to 7 μm with well-defined grain boundaries. In this way, the average grain size changes from ~6.8 ± 3.6 μm in the sample without additives to 6.2±2.4, 5.6±3.9 and 5.3 ± 3.2μm for samples obtained using CTAB, HMTA and Triton, respectively.

The high density ceramic is perfectly adapted to measure the dielectric and ferroelectric properties. Concerning the electrical properties of sintered samples, real permittivity (ε') and dielectric loss (tan(δ)) curves are shown in Figures 5(a) and (b), respectively, as a function of frequency and reaction conditions. These results are also summarized in Table 1, and it can be seen that samples obtained using additives presented dielectric constant values similar to $K_{0.5}Na_{0.5}NbO_3$ [21], whereas the sample obtained using Triton X-100 showed the highest dielectric constant. In general, losses and real permittivity decrease with frequency due to Debye effect, however this behaviour is more pronounced for the sample obtained using CTAB. The increase of ε' and tan(δ) at low frequencies for polar materials is attributed from the contribution of multicomponent polarization mechanisms (i.e. electronic, ionic, orientation and space charge) [22]. At high frequencies the dipoles cannot rotate rapidly, so that their oscillations lag behind those of the field [23]. As the frequency is further increased, the dipole will be completely unable to follow the field and the orientation polarization ceases, so ε' decreases reaching a constant value at high frequencies due to interfacial polarization [24].

The temperature dependence of the dielectric constant (real permittivity) and the dielectric loss of samples obtained using

different additives are shown in Figs. 6 (a) and (b), respectively. The dielectric properties were measured over a wide temperature range from 25ºC to 500ºC at different frequencies. Peak anomalies of the dielectric constant are shown at about 380ºC and 270ºC. These transition temperatures could be related to the monoclinic-orthorhombic phase transition observed at ~270ºC and orthorhombic-tetragonal phase transition registered at 365ºC, respectively. The obtained values for samples synthesized without additives are closer to transformation temperatures of $NaNbO_3$ than of $KNbO_3$, suggesting that these ceramics have a high concentration of $NaNbO_3$ or that $x<0.5$ in $K_xNa_{1-x}NbO_3$ [25]. On the other hand, Curie temperatures clearly moved to higher values in systems obtained using modifiers, suggesting that these additives increase the K incorporation into the structure during the synthesis process.

Sintered samples were analysed under an external strong electric field, exhibiting ferroelectric behaviour due to spontaneous polarization in all cases. The polarization hysteresis loop of KNN ceramics at room temperature and under different electric field (up to E_p = 70kV/cm) are shown in Fig. 7. All samples showed well-saturated shape curves. Samples prepared without additives showed a coercive electric field (E_c) of 34kV/cm, a saturation polarization of 16μC/cm^2, and high remnant polarization (P_r) of 11μC/cm^2, whereas samples prepared using surface modified showed similar E_c values (~30 kV/cm), although CTAB, HMTA and Triton showed different P_r and P_s values (10, 11 and 8 μC/cm^2 and 13, 17 and 12 μC/cm^2, respectively). It can be seen that CTAB and Triton are a softening modifiers, demonstrate a profound effect of it dopants on the shape of the P-E hysteresis loop. Although the d_{33} values registered in all samples are lower than that measured in pure $K_{0.5}Na_{0.5}NbO_3$ obtained by solid-state reaction, piezoelectric properties were increased with the potassium incorporation in the structure (Table 1).

It was established that the presence of CTAB, HMTA or Triton X-100 during the hydrothermal synthesis of $K_xNa_{(1-x)}NbO_3$ improve the electrical properties of this material by increasing the K content in the lattice. Further studies are necessary in order to determine the mechanisms of action of each additive.

Conclusion

Microstructural and electrical properties of $K_xNa_{1-x}NbO_3$ obtained by hydrothermal synthesis and using different surface modifiers, NaOH/KOH ratio of 0.6 and total hydroxide concentration 8N have been studied. The following conclusions are derived from this study.

- The XRD patterns showed that sodium-rich compositions in agreement with the $K_{0.10}Na_{0.90}NbO_3$ along with $K_{0.65}Na_{0.35}NbO_3$ were obtained. The K concentration in the lattice increased significantly due to additive effects.
- Sintered samples obtained from solution using different surface modifiers showed improved dielectric behavior and piezoelectric properties. Dielectric constants of samples obtained using additives were similar to that of $K_{0.5}Na_{0.5}NbO_3$.

- Curie temperature of samples prepared using Triton X100 was near to that of $K_{0.5}Na_{0.5}NbO_3$. Also, these samples present higher tetragonality and dielectric properties.

Acknowledgements

This work is carried out with funds from CONICET, ANPCyT, University of Mar del Plata (Argentina) and MINECO (Spain) (project MAT2013-48009-C4-1-P). Dr. F. Rubio-Marcos is also indebted to MINECO for a ''Juan de la Cierva'' contract (ref: JCI-2012-14521), which is co-financed with FEDER funds.

References

[1] J. Rodel, W. Jo, K. T. P. Seifert, E. M Anton, T. Granzow, D. Damjanovic, J. Am. Ceram. Soc. 92, 1153 (2009).

[2] X.P. Jiang, L.Z. Li, M. Zeng, H.L.W. Chan, Mater. Lett. 60, 1786 (2006).

[3] M.D. Maeder, D. Damjanovic, N. Setter, J. Electroceram. 13, 385 (2004).

[4] L. Li, Y.-Q. Gong, L.-J. Gong, H. Dong, X.-F. Yi, X.-J. Zheng, Mater. Design, 33, 362 (2012).

[5] L. Bai, K. Zhu, L. Su, J. Qiu, H. Ji, Mater. Lett. 64, 77 (2010).

[6] J.T. Zeng, K.W. Kwok, H.L.W. Chan, Mater. Lett. 61, 409 (2007).

[7] Y. Xu, D. Liu, F.P. Lai, Y.H. Zhen, J.F. Li, J. Am. Ceram. Soc. 91, 2844 (2008).

[8] W.J. Dawson, Ceram. Bull. 67, 1673 (1988).

[9] G.K.L. Goh, F.F. Lange, S.M. Haile, J. Mater. Res. 18, 338 (2003).

[10] H. Zhu, Z. Zheng, X. Gao, Am. J. Chem. Soc. 128, 2373 (2006).

[11] A. Magrez A, E. Vasco, J.W. Seo, C. Dieker, N. Setter,L. Forró, J. Phys. Chem. 110, 58 (2006).

[12] M. Ishikawa, N. Takiguchi, H. Hosaka, Jpn. J. Appl. Phys. 47, 3824 (2008).

[13] F. Zhang, L. Han, S. Bai, Jpn. J. Appl. Phys. 47, 7685 (2008).

[14] J. Ortiz-Landeros, C. Gómez-Yáñez, R. López-Juárez, I. Dávalos-Velasco, H.Pfeiffer, J. Adv. Ceram. 1, 204 (2012).

[15] S. Bai, F. Zhang, T. Karaki, M. Adachi, Jpn. J. Appl. Phys. 50, 09ND12 (2011).

[16] Y. Xu, D. Liu, F. Lai, Y. Zhen, J.-F. Li, J. Am. Ceram Soc. 91, 2844 (2008).

[17] F. Rubio-Marcos, J.J. Romero, J.F. Fernandez, J. Nanopart. Res. 12, 2495 (2010).

[18] F. Rubio-Marcos, P. Marchet, T. Merle-Méjean, J.F. Fernandez, Mater. Chem. Phys. 123, 91 (2010).

[19] J. Tellier, B. Malic, B. Dkhil, D. Jenko, J. Cilensek, M. Kosec, Solid State Sci. 11, 320 (2009).

[20] F. Rubio-Marcos, M.A. Bañares, J.J. Romero, J.F. Fernández, J. Raman Spectrosc. 42, 639 (2011).

[21] L.A. Ramajo, J. Taub, M.S. Castro, Materials Research 17, 728 (2014).

[22] N.A. Hegab, A.E. Bekheet, M.A. Afifi, L.A. Wahaba, H.A. Shehata, J. Ovonic Res. 3, 71 (2007).

[23] K.K. Srivaslava, A. Kumar, O.S. Panwar, K.N. Lakshminarayan, J. Non-Cryst. Solids 33, 205 (1979).

[24] E. A. Zereffa, A. V. Prasadarao, Int. Res. J. Pure Appl. Chem. 2, 130 (2012).

[25] N. Zhang, A.M. Glazer, D. Baker, P.A. Thomas, Acta Cryst. B 65, 291 (2009).

Figure Captions

Figure 1. Influence of the different additives in the structure of the KNN obtained by hydrothermal process: XRD patterns of KNN samples and detail of the 45.5º to 47.5º 2θ range.

Figure 2. (a) Raman spectra of KNN obtained using different additives, with a constant NaOH/KOH ratio of 0.6 and a 8N total hydroxide concentration. (b) Position of the ν_1 and ν_2 bands as a function of additives. **The error bars show the standard deviation (sd) of the Raman shift evolution of the ν_1 and ν_2 bands for each sample.**

Figure 3. (a-d) SEM images of samples synthesized using a) 8N OH^- solution, b) Triton X-100, c) CTAB, and d) HMTA; e) Potassium concentration of $K_xNA_{1-x}NbO_3$ synthesized with different additives. **Scale bar, 2 µm**

Figure 4. SEM images of samples synthesized using a) 8N, b) Triton X-100, c) CTAB, and d) HMTA. **Scale bar, 5 µm**

Figure 5. Variation of the relative permittivity (a) and (b) loss tangent (tan(δ)) as a function of frequency for samples synthesized using different additives.

Figure 6. Relative permittivity (*top*) and dielectric loss (*bottom*) as a function of frequency and temperature for samples synthesized using different surface modifiers (CTAB, HTMA and Triton) with total hydroxide concentrations equal to 8N with a 0.6 NaOH/KOH ratio.

Figure 7. Hysteresis loops at room temperature for samples obtained using different surfaces modified a) 8N; b) CTAB; c) HTMA and d) Triton.

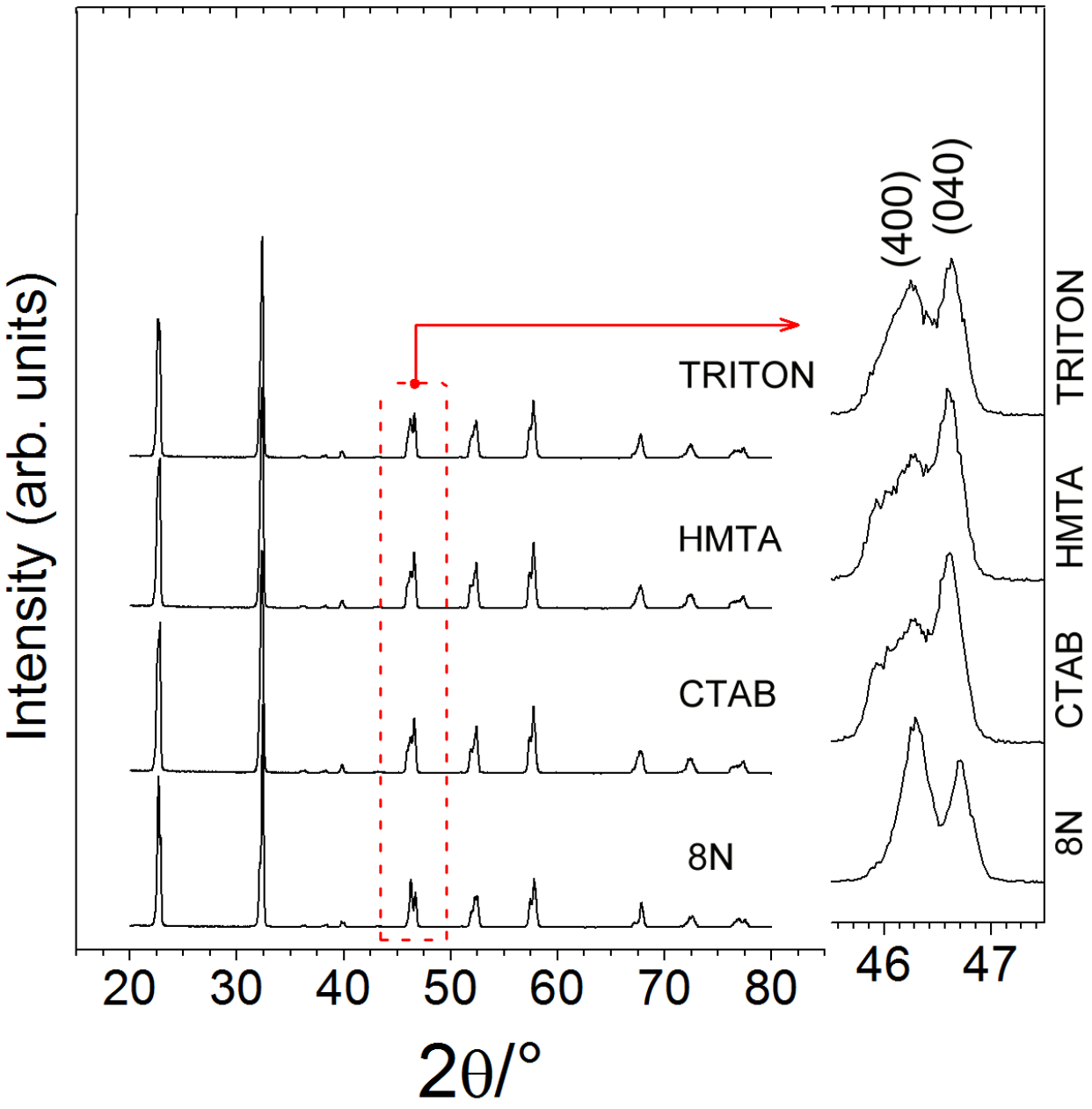
Intensity (arb. units)
TRITON
HMTA
CTAB
8N
20
30
40
50
60
70
80
2θ/°
(400)
(040)
46
47

Figure 1

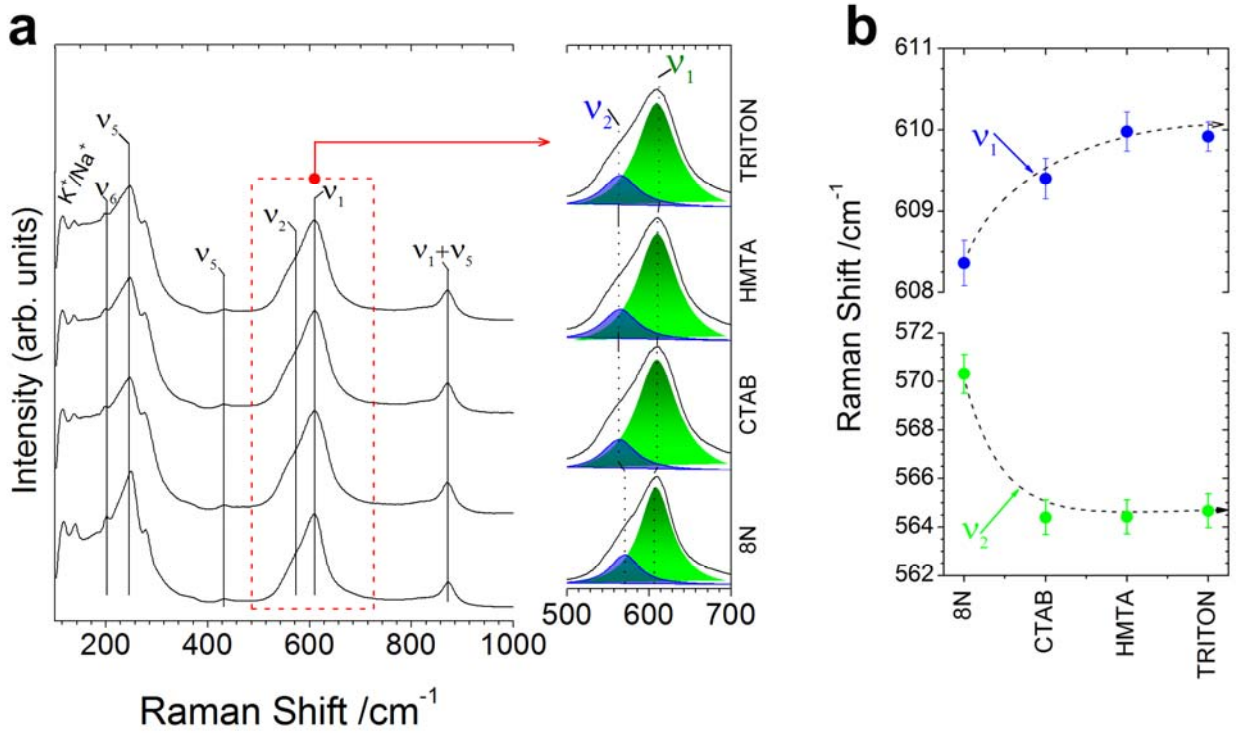
a
b
Intensity (arb. units)
Raman Shift /cm-1
K+/Na+
ν5
ν6
ν2
ν1
ν1+ν5
TRITON
HMTA
CTAB
8N
200
400
600
800
1000
500
600
700
611
610
609
608
572
570
568
566
564
562
Raman Shift /cm-1
8N
CTAB
HMTA
TRITON

Figure 2

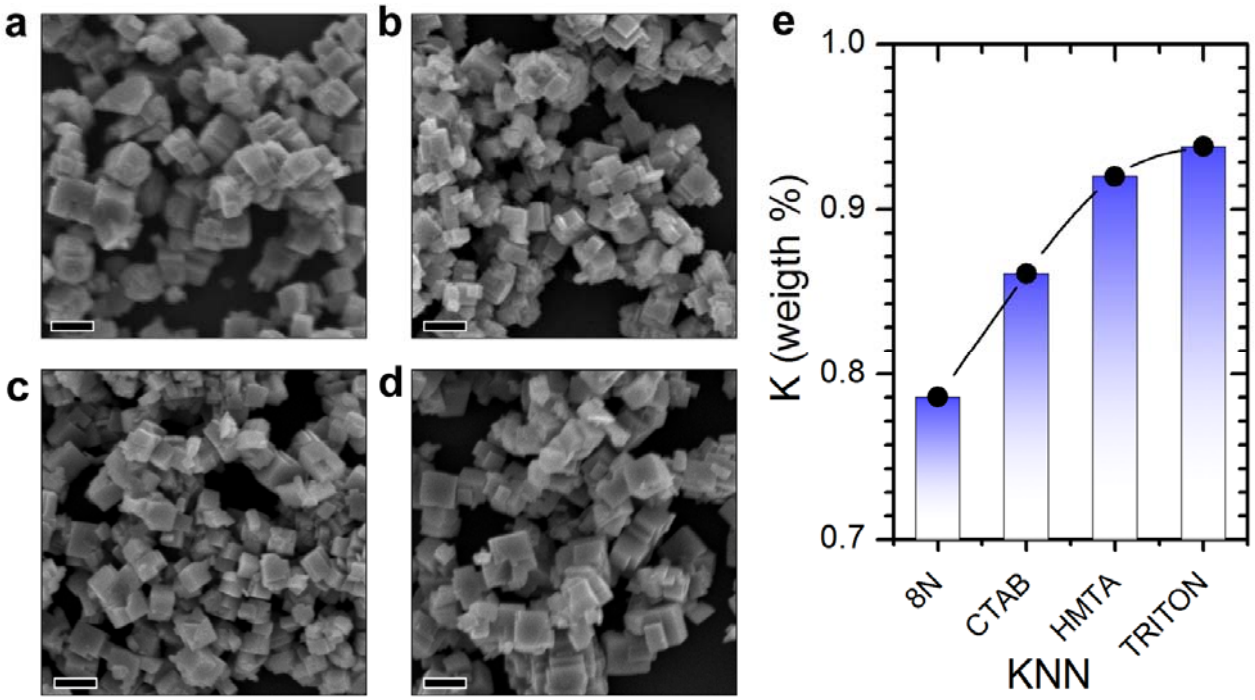

Figure 3

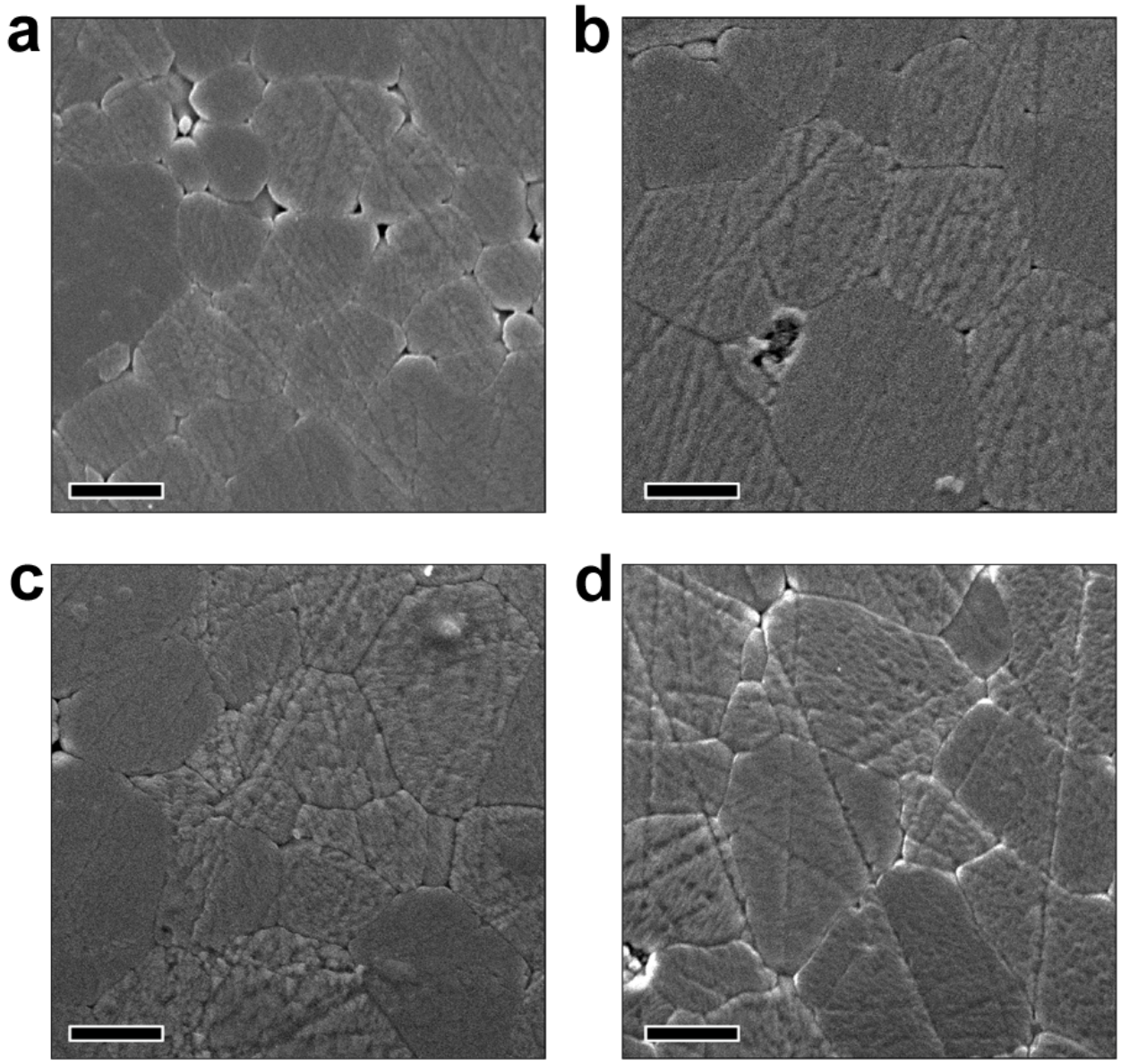

Figure 4

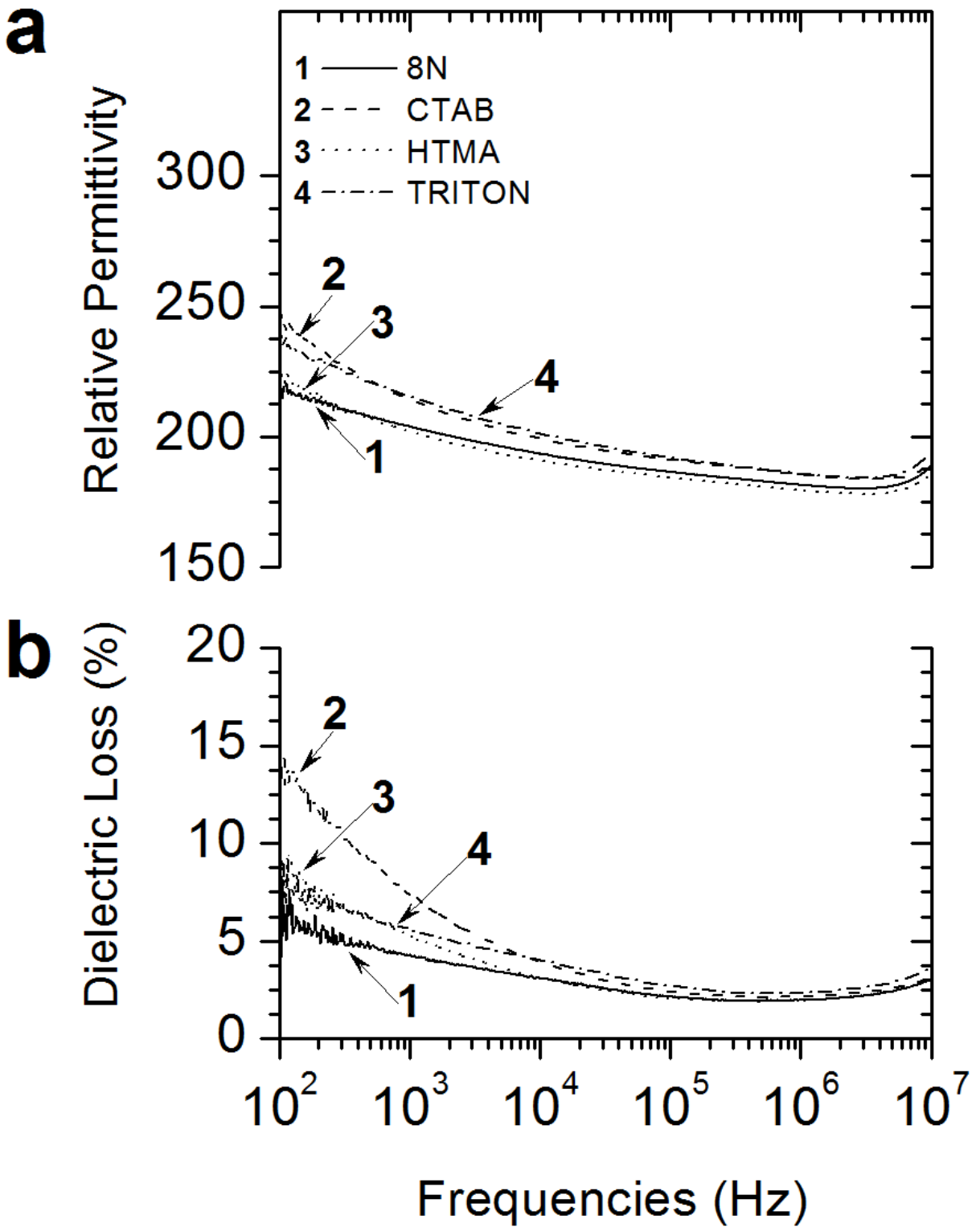
a
1 8N
2 CTAB
3 HTMA
4 TRITON
Relative Permittivity
300
250
200
150
2
3
4
1
b
Dielectric Loss (%)
20
15
10
5
0
2
3
4
1
10^2 10^3 10^4 10^5 10^6 10^7
Frequencies (Hz)

Figure 5

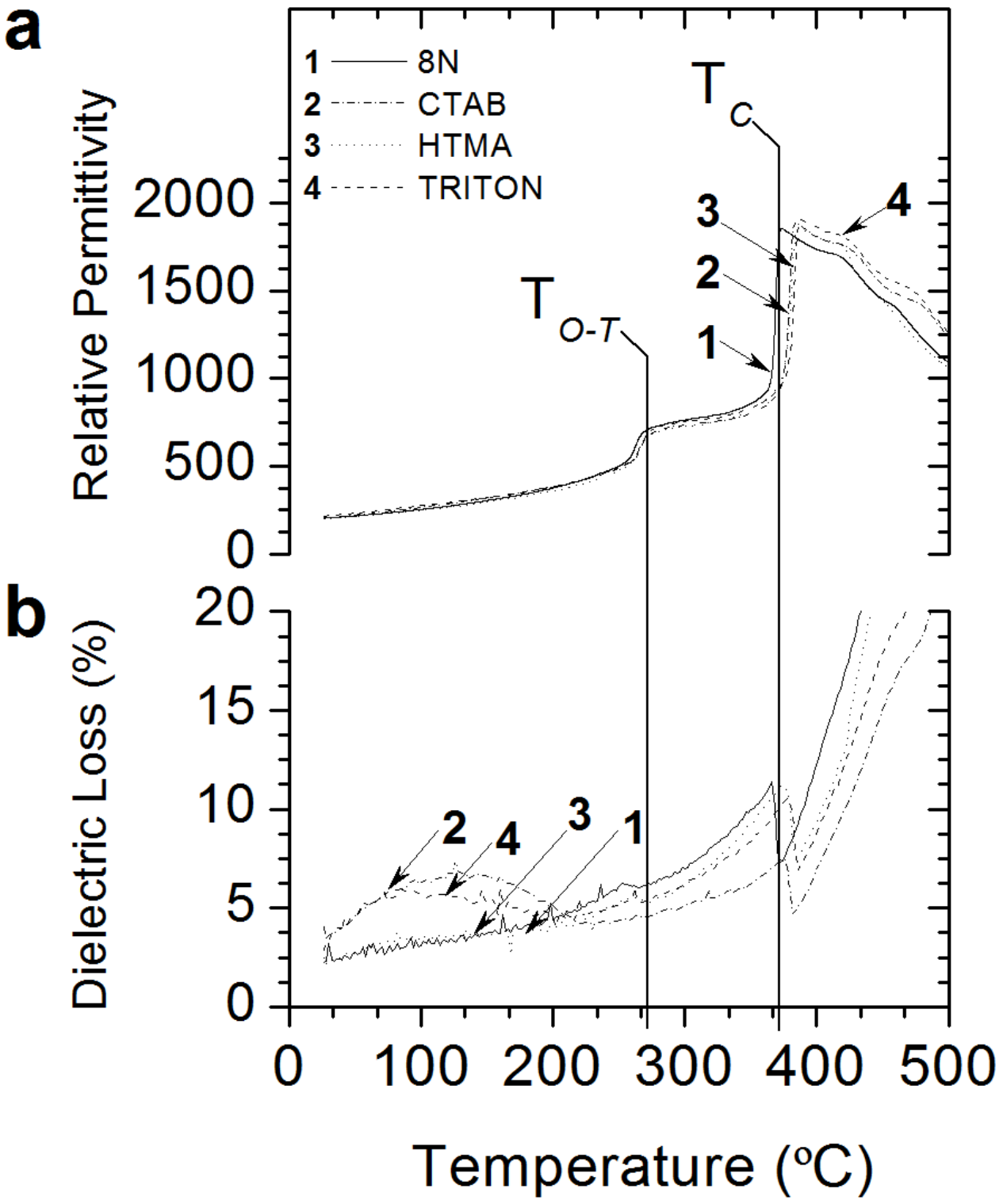
a
b
1 8N
2 CTAB
3 HTMA
4 TRITON
Relative Permittivity
2000
1500
1000
500
0
T C
T O-T
1
2
3
4
Dielectric Loss (%)
20
15
10
5
0
0 100 200 300 400 500
Temperature (°C)

Figure 6

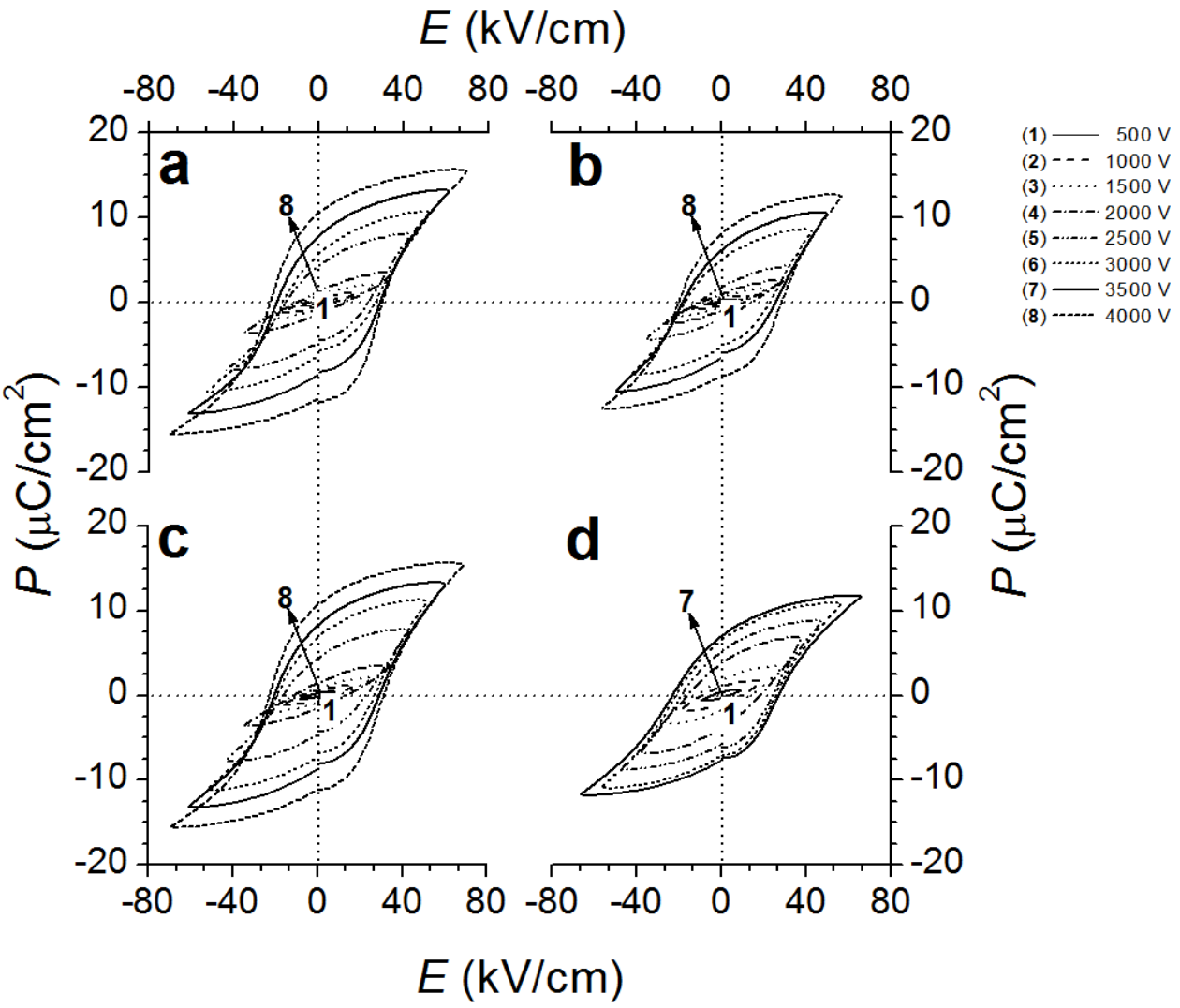
E (kV/cm)
P (μC/cm²)
a
b
c
d
(1) 500 V
(2) 1000 V
(3) 1500 V
(4) 2000 V
(5) 2500 V
(6) 3000 V
(7) 3500 V
(8) 4000 V

Figure 7

Table 1. Apparent density (ρ), mean grain size (d_{50}), real permittivity (ε') and loss tangent (tan(δ)) at 10 kHz and room temperature of KNN samples obtained under different surface additives and pure $K_{0.5}Na_{0.5}NbO_3$ obtained by solid-state reaction [21].

Sample	**ρ (g/cm^3)**	**d_{50} (μm)**	**ε'**	**tan (δ)**	**d_{33} (μC/cm)**
8N	4.33 ± 0.05	6.8±3.6	176	0.032	45 ± 5
CTAB	4.30 ± 0.01	6.2±2.4	387	0.037	56 ± 6
HMTA	4.29 ± 0.02	5.6±3.9	381	0.029	60 ± 6
TRITON	4.23 ± 0.02	5.3±3.2	397	0.028	61 ± 6
$K_{0.5}Na_{0.5}NbO_3$	4.28 ± 0.19	1.6±1.1	352	0.13	86 ± 6